

## Synthesis of a Soluble Precursor Possessing an Nb–N Backbone Structure and Its Pyrolytic Conversion into Niobium-Based Ceramics

Fei Cheng, Yoshiyuki Sugahara,\* and Kazuyuki Kuroda†

Department of Applied Chemistry, School of Science and Engineering, Waseda University, Ohkubo-3, Shinjuku-ku, Tokyo 169-8555

†Kagami Memorial Laboratory for Materials Science and Technology, Waseda University, Nishiwaseda-2, Shinjuku-ku, Tokyo 169-0051

(Received December 1, 1999)

Synthesis and pyrolysis of a soluble precursor possessing an Nb–N backbone structure were investigated. The precursor was prepared by aminolysis reaction of tetrakis(diethylamido)niobium with isopropylamine. The precursor was soluble in benzene, and had a polymeric structure possessing Nb–N–Nb imido-bridges. The precursor was pyrolyzed under  $\text{NH}_3\text{--N}_2$  (at 600 °C for 2 h under  $\text{NH}_3$  and subsequently at 1350 °C for 8 h under  $\text{N}_2$ ) and Ar (at 1500 °C for 2 h) atmospheres.  $\delta\text{-NbN}$  was obtained as a main crystalline phase after the pyrolysis of the precursor under  $\text{NH}_3\text{--N}_2$ , whereas pyrolysis of the precursor under Ar led to the formation of NbC as the only crystalline phase. More than 90% of niobium which was present in the precursor remained in both of the pyrolyzed products.

Niobium nitride has attracted considerable attention because of its desirable properties; these include hardness, thermal stability, and, particularly in the case of cubic form, superconductivity.<sup>1</sup> Niobium nitride has several phases:  $\delta\text{-NbN}$ ,  $\gamma\text{-NbN}$ ,  $\varepsilon\text{-NbN}$ ,  $\beta\text{-Nb}_2\text{N}$ , and  $\text{Nb}_3\text{N}_4$ . However, all of these phases except  $\delta\text{-NbN}$  have hexagonal structures.<sup>2,3</sup> The structure of  $\delta\text{-NbN}$  is B1(NaCl)-type where the bonding character between Nb and N is metallic.<sup>1</sup> The  $\delta\text{-NbN}$  is a superconductor with  $T_c$  of 17.3 K, and has been used in various devices such as dc-superconducting quantum interference devices, Josephson junctions, and switches for pulsed power applications.<sup>1,4,5</sup> The conventional synthetic procedure of NbN is direct nitridation of Nb metal at high temperature and high  $\text{N}_2$  pressure.<sup>1,3</sup> Chemical vapor deposition (CVD) processes have also been widely investigated for the preparation of NbN films.<sup>2,6–8</sup>

Pyrolytic conversion of precursors has been widely applied to the preparation of carbides and nitrides of various main group elements and transition metals, such as SiC,  $\text{Si}_3\text{N}_4$ , BN, AlN, and TiN.<sup>9–12</sup> Although this chemical route provides a method for the preparation of non-oxide ceramics with desirable shapes, such as coatings and fibers, it is required for such applications that the precursors are soluble or fusible.<sup>10</sup> NbN has been prepared by direct ammonolysis of the niobium halides or niobium dialkylamides and subsequent pyrolysis of the resultant polymeric compounds.<sup>13–15</sup> A NbN precursor has also been prepared recently by an electrochemical route in which metallic niobium was anodically dissolved in a liquid- $\text{NH}_3$  containing  $\text{NH}_4\text{Br}$  solution.<sup>16,17</sup> However, since the precursors prepared by these techniques have highly cross-linked structures, they are insoluble in an

organic solvent such as pentane,<sup>15</sup> pyridine,<sup>15</sup> and acetonitrile.<sup>16,17</sup> As far as we know, the synthesis and pyrolytic conversion of soluble NbN precursors have not been reported.

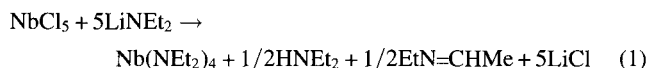
Aminolysis reactions of a number of transition metal dialkylamides of group 4 ( $\text{M}(\text{NR}_2)_4$ ), typically  $\text{Ti}(\text{NR}_2)_4$  ( $\text{R} = \text{Me}$  or  $\text{Et}$ ), with primary amine  $\text{R}'\text{NH}_2$  have been extensively investigated.<sup>18–20</sup> Since primary amines are bifunctional, the aminolysis reactions usually occur with the formation imido-bridge ( $\text{M--N--M}$ ) structures in the aminolysis products. This chemical route provides a possible way to prepare soluble precursors because the formation of highly cross-linked structures can be suppressed by the introduction of organic groups into the aminolysis products. However, insoluble products will form if the steric hindrance of  $\text{R}'$  groups is too small.<sup>18</sup> The reaction of  $\text{Ti}(\text{NET}_2)_4$  with  $\text{Pr}^n\text{NH}_2$  gave an insoluble  $\text{Ti}(\text{NPr}^n)_2$ , while the reaction with  $\text{Bu}^n\text{NH}_2$  led to the formation of a soluble product with a proposed formula of  $\text{Ti}_x(\text{NBu}^n)_{2x-2}(\text{NET}_2)_4$ .<sup>18</sup> A number of aminolysis products have been applied to the preparation of TiN or Ti(N,C).<sup>19–21</sup> However, no aminolysis reactions of transition metal dialkylamides of group 5 with a primary amine and the pyrolytic conversion of the aminolysis products have been studied yet.

In this research, a precursor possessing an Nb–N backbone structure was prepared by an aminolysis reaction of tetrakis(diethylamido)niobium ( $\text{Nb}(\text{NET}_2)_4$ ) using isopropylamine ( $\text{Pr}^i\text{NH}_2$ ). Since isopropyl groups are branched, it is expected that the aminolysis reaction of  $\text{Nb}(\text{NET}_2)_4$  will lead to the formation of a soluble product. Pyrolytic conversion of the precursor was investigated, and the pyrolyzed products were characterized by compositional analysis, X-ray powder diffraction (XRD) and scanning electron microscopy (SEM).

## Experimental

All the procedures were performed under a protective nitrogen atmosphere using the standard Schlenk technique<sup>22</sup> or in a glove box filled with nitrogen. The solvents, *n*-pentane and benzene, were freshly distilled over sodium/benzophenone prior to use. Diethylamine and isopropylamine were freshly distilled over potassium hydroxide prior to use. Niobium chloride (NbCl<sub>5</sub>) was used as received.

**1 Synthesis of Nb(NEt<sub>2</sub>)<sub>4</sub>.** Tetrakis(diethylamido)niobium (Nb(NEt<sub>2</sub>)<sub>4</sub>) was prepared according to the following reaction based on the previous report:<sup>23</sup>



Distillation of the obtained red viscous liquid gave a purple-brown viscous liquid product (bp 120 °C at 13.3 Pa). The IR spectrum (Fig. 1) of the distilled product shows the presence of a  $\nu(\text{Nb-N})$  band at 583 cm<sup>-1</sup> (as shown by arrow) and two  $\nu(\text{NC}_2)$  bands at 1001 and 1154 cm<sup>-1</sup>, consistent with those in the previous report for Nb(NEt<sub>2</sub>)<sub>4</sub>.<sup>24</sup> Elemental analysis exhibits an empirical formula of NbN<sub>4.1</sub>C<sub>16.0</sub>H<sub>38.2</sub> (Table 1), which approximately corresponds to Nb(NEt<sub>2</sub>)<sub>4</sub>. The mass spectrum of the product was consistent with a previous report for the formation of Nb(NEt<sub>2</sub>)<sub>4</sub>:<sup>25</sup> *m/z* (M<sup>+</sup>, EI), 381 (Nb(NEt<sub>2</sub>)<sub>4</sub><sup>+</sup>, 20), 380 (Nb(NEt<sub>2</sub>)<sub>3</sub>[NEt(C<sub>2</sub>H<sub>4</sub>)]<sup>+</sup>, 32), 352 (Nb(NEt<sub>2</sub>)<sub>3</sub>(NEt)<sup>+</sup>, 43), 337 (Nb(NEt<sub>2</sub>)<sub>3</sub>(NCH<sub>2</sub>)<sup>+</sup>, 43), 276 (Nb[NEt(CH=CH<sub>2</sub>)<sub>2</sub>](NEt)<sup>+</sup>, 58), and 58 (EtNCH<sub>3</sub><sup>+</sup>, 100).

Table 1. Compositional Characteristics of the Nb(NEt<sub>2</sub>)<sub>4</sub> and the Precursor

	Elemental analysis/mass%					Empirical formula
	Nb	N	C	H	Total	
Nb(NEt <sub>2</sub> ) <sub>4</sub>	24.2	14.8	49.9	9.9	98.8	NbN <sub>4.0</sub> C <sub>16.0</sub> H <sub>38.2</sub>
Precursor	35.5	14.2	37.6	8.1	95.4	NbN <sub>2.6</sub> C <sub>8.1</sub> H <sub>21.1</sub>

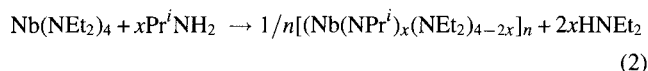
However, although Nb(NEt<sub>2</sub>)<sub>4</sub> does not show any signal in the NMR spectrum because of its paramagnetic property, the <sup>1</sup>H NMR spectrum of this viscous product showed the presence of small amounts of two diamagnetic compounds, tris(diethylamido)ethyl-imidoniobium (Et<sub>2</sub>N)<sub>3</sub>Nb(=NEt) and tris(diethylamido)azapentane-

2,3-diylniobium (Et<sub>2</sub>N)<sub>3</sub>Nb(EtNCHMe)<sup>26</sup> (The <sup>1</sup>H NMR data obtained in this study are shown in References). The presence

of (Et<sub>2</sub>N)<sub>3</sub>Nb(=NEt) and (Et<sub>2</sub>N)<sub>3</sub>Nb(EtNCHMe) as minor components in distilled Nb(NEt<sub>2</sub>)<sub>4</sub> was also reported previously.<sup>7,26</sup>

Because only small amounts of (Et<sub>2</sub>N)<sub>3</sub>Nb(=NEt) and (Et<sub>2</sub>N)<sub>3</sub>Nb(EtNCHMe) were present in the viscous product according to the elemental analysis, we will hereafter refer to the viscous product simply as Nb(NEt<sub>2</sub>)<sub>4</sub>, which was used as a starting material of the precursor.

**2 Synthesis of a Precursor.** The polymeric precursor possessing an Nb-N backbone structure was prepared based on a previous report,<sup>27</sup> by the reaction of Nb(NEt<sub>2</sub>)<sub>4</sub> with an excess of isopropylamine (Nb : Pr<sup>*i*</sup>NH<sub>2</sub> = 1 : 5). An ideal reaction can be expressed by Eq. 2:



Nb(NEt<sub>2</sub>)<sub>4</sub> was dissolved in 30 mL of benzene in a 100 mL three-necked flask, and Pr<sup>*i*</sup>NH<sub>2</sub> in 20 mL of benzene was slowly dropped into the Nb(NEt<sub>2</sub>)<sub>4</sub> solution at about 10 °C with stirring. The mixed solution was stirred for 2 h at 10 °C. Then the resultant solution was gradually heated, and finally refluxed at 78 °C for 16 h. A dark brown solid, which was completely soluble in benzene, was obtained after benzene was removed under reduced pressure.

**3 Pyrolysis.** The precursor was pyrolyzed in a tube furnace. About 0.5 g of precursor was placed in an Al<sub>2</sub>O<sub>3</sub> boat, which was

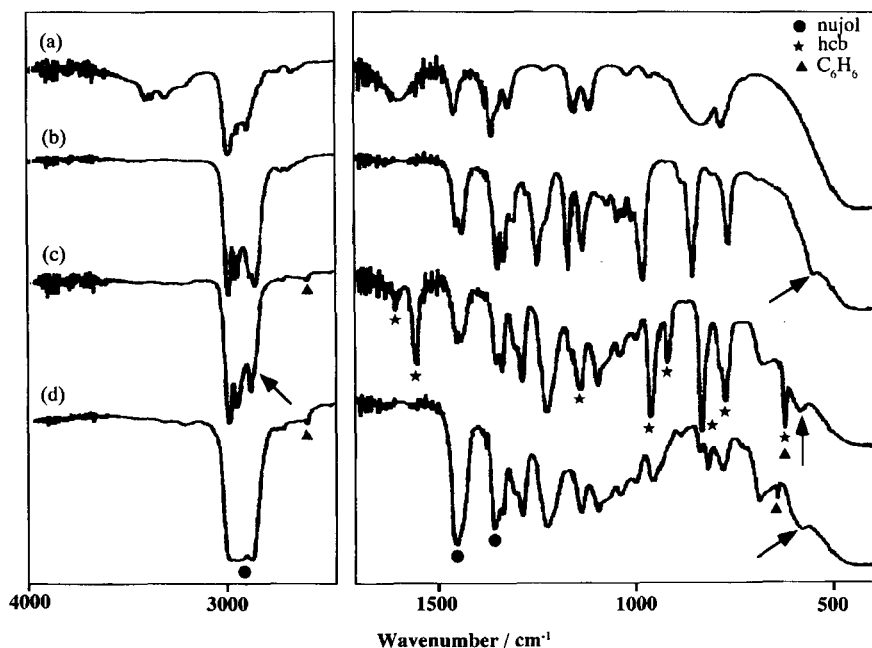


Fig. 1. IR spectra of (a) Pr<sup>*i*</sup>NH<sub>2</sub>, (b) Nb(NEt<sub>2</sub>)<sub>4</sub>, (c) precursor (hcb technique), and (d) precursor (nujol technique). The meaning of the arrows is prescribed in the text.

then introduced into an  $\text{Al}_2\text{O}_3$  tube filled with Ar or  $\text{NH}_3$ . For pyrolysis under  $\text{NH}_3\text{--N}_2$ , the precursor was first heated at  $600^\circ\text{C}$  for 2 h under  $\text{NH}_3$  with a flow rate of  $30\text{ mL min}^{-1}$ , and cooled to room temperature. Then, the resultant product was heated again at  $1350^\circ\text{C}$  for 8 h under  $\text{N}_2$  ( $100\text{ mL min}^{-1}$ ). For pyrolysis under Ar, the precursor was heated at  $1500^\circ\text{C}$  for 2 h with a flow rate of  $100\text{ mL min}^{-1}$ .

**4 Analyses.** The precursor was characterized by infra-red spectroscopy (IR, Perkin–Elmer FTIR-1640, with nujol technique and hexachloro-1,3-butadiene (hcb) technique). The amounts of nitrogen, carbon, and hydrogen in the precursor were measured by using a Perkin–Elmer PE2400 instrument. The pyrolysis behavior of the  $\text{Nb}(\text{NEt}_2)_4$  and the precursor was investigated by thermogravimetry-mass spectrometry (TG-MS) (Shimadzu TGA-50 thermobalance coupled with a Shimadzu QP1100EX quadrupole mass spectrometer via a stainless capillary). In order to identify the evolved gases clearly,  $\text{Nb}(\text{NEt}_2)_4$  and the precursor were pyrolyzed using a tube furnace under a He flow; the evolved gases trapped using liquid nitrogen in a certain temperature range were identified by gas chromatography-mass spectrometry (GC-MS) (Hewlett-Packard Model 5890 Series II Gas Chromatograph coupled with a 5971A Mass Selective Detector; the separation was performed on a capillary column (Chrompack Pora Plot Q, for the gases from  $\text{Nb}(\text{NEt}_2)_4$ ) or a capillary column (GL Science TC-5, for the gases from the precursor)). The pyrolyzed products were analyzed by X-ray powder diffraction (XRD,  $\text{Cu K}\alpha$ ; Mac Science MXP3). The lattice parameters of the pyrolyzed products were calculated by the non-linear least-squares method. The amounts of nitrogen, oxygen and carbon in the pyrolyzed products were measured by using LECO TC-436 and CS-444LS instruments. The amounts of niobium in the precursor and the pyrolyzed products were determined by inductively coupled plasma emission spectroscopy (ICP, Nippon Jarrell Ash ICAP-575 II), after the samples were dissolved with a mixed solution of 10 mL of HF, 5 mL of  $\text{H}_2\text{SO}_4$ , and 5 mL of  $\text{HNO}_3$  at  $200^\circ\text{C}$  for 2 h. The morphology of the pyrolyzed products was investigated by scanning electron microscopy (SEM, Hitachi S4500-S).

## Results and Discussion

**1 Preparation of a Soluble Precursor via Aminolysis of  $\text{Nb}(\text{NEt}_2)_4$ .** The IR spectrum of the precursor, as well as those of the  $\text{Nb}(\text{NEt}_2)_4$  and isopropylamine, are shown in Fig. 1. The IR spectrum of  $\text{Nb}(\text{NEt}_2)_4$  shows four strong (C–H) bands at  $2963$ ,  $2926$ ,  $2865$ , and  $2834\text{ cm}^{-1}$ , which are assigned to  $\nu_{\text{as}}(\text{CH}_3)$ ,  $\nu_{\text{as}}(\text{CH}_2)$ ,  $\nu_{\text{s}}(\text{CH}_3)$ , and  $\nu_{\text{s}}(\text{CH}_2)$  modes of the ethyl groups respectively (Fig. 1b).<sup>28</sup> On the other hand, the IR spectrum of the precursor (Fig. 1c) shows three strong (C–H) bands assignable to  $\nu_{\text{as}}(\text{CH}_3)$ ,  $\nu(\text{CH})$ , and  $\nu_{\text{s}}(\text{CH}_3)$  modes of isopropyl group at  $2960$ ,  $2908$ , and  $2861\text{ cm}^{-1}$ , respectively; only a weak shoulder band assignable to  $\nu_{\text{s}}(\text{CH}_2)$  modes of ethyl groups is present at around  $2832\text{ cm}^{-1}$  (as shown by the arrow).<sup>28</sup> In addition, in the spectrum of the precursor, the bands at  $1155$  and  $1111\text{ cm}^{-1}$  due to  $-\text{CH}(\text{CH}_3)_2$  skeletal bands<sup>28</sup> are clearly observed. All of these observations indicate that a large portion of the  $\text{NEt}_2$  (and  $\text{NEt}$ ) groups in the starting material has been substituted with  $\text{NPr}^i$  groups. Besides, in the IR spectrum of the precursor (Fig. 1c), the  $\nu(\text{Nb--N})$  band of  $\text{Nb}(\text{NEt}_2)_4$  (at  $583\text{ cm}^{-1}$  as shown by arrow in Fig. 1b) disappears, and a new band assignable to  $\nu(\text{Nb--N})$  appears at  $613\text{ cm}^{-1}$  (as

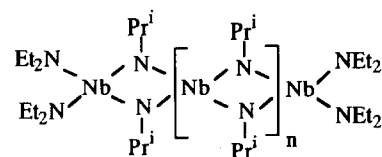
shown by the arrow). Because no band is observed at the typical frequency region of  $\nu(\text{N--H})$  ( $3300\text{--}3500\text{ cm}^{-1}$ )<sup>28</sup> in the spectrum of the precursor, Nb–N–Nb imido-bridges should have formed.

The elemental analysis results of the precursor are shown in Table 1. The N:C:H molar ratio of the precursor is 1:3.1:8.1, close to that of  $\text{NPr}^i$  group (1:3:7), indicating that a large portion of the  $\text{NEt}_2$  groups (1:4:10) in  $\text{Nb}(\text{NEt}_2)_4$  has been substituted with  $\text{NPr}^i$  groups. The N/Nb molar ratio decreases from 4 for the  $\text{Nb}(\text{NEt}_2)_4$  to 2.6 for the precursor, which is consistent with the IR results showing that the nitrogen atoms in the  $\text{NPr}^i$  groups are present as Nb–N–Nb imido-bridges. The empirical formula of  $\text{NbN}_{2.6}\text{C}_{8.1}\text{H}_{21.1}$  indicates that, besides the  $\text{NPr}^i$  groups, a small amount of  $\text{NEt}_2$  groups should remain in the precursor (assuming that N and C belong to either  $\text{NPr}^i$  or  $\text{NEt}_2$  groups), also consistent with the IR results. Bradley et al.<sup>18</sup> reported that the aminolysis of  $\text{Ti}(\text{NEt}_2)_4$  with *n*-butylamine led to the formation of a soluble polymer due to the presence of a small amount of  $\text{NEt}_2$  groups as chain stoppers. Hence, it is also probable that the presence of a small amount of  $\text{NEt}_2$  groups as chain stoppers led to the formation of a soluble polymer with a postulated structure as shown in Scheme 1.

**2 Pyrolysis of the Precursor.** The pyrolysis behavior of the precursor was investigated by using TG-MS. The pyrolysis behavior of  $\text{Nb}(\text{NEt}_2)_4$  was also studied for comparison. The TG curves and the temperature profiles of the selected fragments are shown in Fig. 2. The ceramic yields of  $\text{Nb}(\text{NEt}_2)_4$  and the precursor up to  $900^\circ\text{C}$  are 37 and 57% respectively, indicating the advantage of the polymeric structure of the precursor.

In the TG curve of the  $\text{Nb}(\text{NEt}_2)_4$ , a sharp mass loss is observed in the temperature range of ca.  $160\text{--}280^\circ\text{C}$ . Gas (in the trap-tube), liquid (near the outlet of the tube furnace and in the trap-tube), and a small amount of yellow solid (near the outlet of the tube furnace) were obtained during the pyrolysis of the  $\text{Nb}(\text{NEt}_2)_4$  using a tube furnace in the corresponding temperature range (ca.  $160\text{--}280^\circ\text{C}$ ). GC-MS (for gas) and  $^1\text{H NMR}$  (for liquid) analyses showed that  $\text{C}_2\text{H}_4$ ,  $\text{C}_2\text{H}_6$ ,  $\text{C}_3\text{H}_6$ ,  $\text{C}_4\text{H}_8$ ,  $\text{CH}_3\text{CN}$ , and  $\text{HNEt}_2$  were the main species evolved. ICP analysis showed that the condensed yellow solid contained Nb.

The temperature profiles for the pyrolysis of the  $\text{Nb}(\text{NEt}_2)_4$  show that fragments at  $m/z$  58 (arising from  $\text{HNEt}_2$ ),  $m/z$  27 (arising from  $\text{C}_2\text{H}_4$  and  $\text{C}_2\text{H}_6$ ) and  $m/z$  41 (arising from higher hydrocarbons ( $\text{C}_n\text{H}_{2n}$  and  $\text{C}_n\text{H}_{2n+2}$ ,  $n \geq 3$ ; e.g.,  $\text{C}_3\text{H}_6$ ,  $\text{C}_4\text{H}_8$ , and  $\text{C}_4\text{H}_{10}$ ) and  $\text{CH}_3\text{CN}$ ) are clearly detected in the temperature range of ca.  $160\text{--}280^\circ\text{C}$  (Fig. 2a).  $\text{Et}_2\text{NH}$  and  $\text{C}_2\text{H}_4$  were reported as the major evolution gases dur-



Scheme 1. The postulated structure of the precursor.

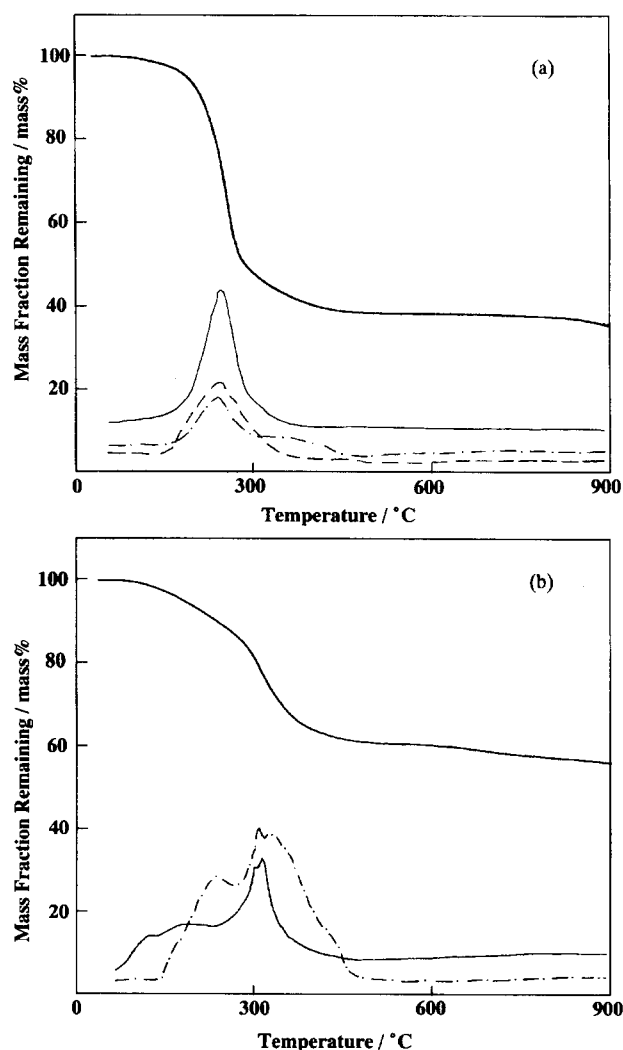
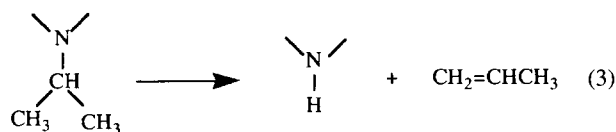


Fig. 2. TG-MS analysis of  $\text{Nb}(\text{NEt}_2)_4$  and the precursor under He. (a) The TG curve of  $\text{Nb}(\text{NEt}_2)_4$ ; the fragment at  $m/z = 58$  arising from  $\text{HNEt}_2$  (—); the fragment at  $m/z = 27$  arising from  $\text{C}_2\text{H}_4$  and  $\text{C}_2\text{H}_6$  (---); the fragment at  $m/z = 41$  arising from higher hydrocarbons ( $\text{C}_n\text{H}_{2n}$  and  $\text{C}_n\text{H}_{2n+2}$ ,  $n \geq 3$ ) and  $\text{CH}_3\text{CN}$  (-·-). (b) The TG curve of the precursor; the fragment at  $m/z = 44$  arising from  $\text{Pr}^i\text{NH}_2$  (—); the fragment at  $m/z = 41$  arising from hydrocarbons ( $\text{C}_n\text{H}_{2n}$  and  $\text{C}_n\text{H}_{2n+2}$ ,  $n \geq 3$ ) and  $\text{CH}_3\text{CN}$  (-·-).

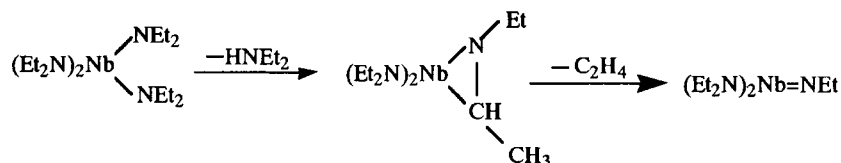
ing the pyrolysis of  $\text{Nb}(\text{NEt}_2)_4$  at  $220^\circ\text{C}$ .<sup>29</sup> The main pyrolysis processes probably involve the elimination of the  $\text{NEt}_2$  groups through the transfer of hydrogen atom from an  $\text{NEt}_2$  group to another one, leading the subsequent formation of a three-membered metallacycle intermediate containing a Nb–C bond (see Scheme 2). Then  $\text{C}_2\text{H}_4$  was released from the three-membered metallacycle intermediate via the

Nb–C bond cleavage. The formation of such a three-membered metallacycle compound has been reported previously for the pyrolysis of diethylamido complexes of Nb, Ta, V, and Ti.<sup>25,30–32</sup>

On the other hand, a large mass loss is observed at the temperature below ca.  $500^\circ\text{C}$  in the TG curve of the precursor (Fig. 2b).  $\text{C}_3\text{H}_6$ ,  $\text{C}_4\text{H}_8$ ,  $\text{CH}_3\text{CN}$ , and  $\text{Pr}^i\text{NH}_2$  were the main species evolved during the pyrolysis of the precursor using the tube furnace below  $500^\circ\text{C}$ . The temperature profiles of the fragments at  $m/z$  44 (arising from  $\text{Pr}^i\text{NH}_2$ ) and  $m/z$  41 (arising from hydrocarbons ( $\text{C}_n\text{H}_{2n}$  and  $\text{C}_n\text{H}_{2n+2}$ ,  $n \geq 3$ ; e.g.,  $\text{C}_3\text{H}_6$ ,  $\text{C}_4\text{H}_8$ , and  $\text{C}_4\text{H}_{10}$ ) and acetonitrile  $\text{CH}_3\text{CN}$ ) are shown in Fig. 2b. The fragment at  $m/z$  44 in the temperature range of ca.  $250$ –ca.  $350^\circ\text{C}$  shows that  $\text{Pr}^i\text{NH}_2$  evolved at this relatively high temperature range. (The evolution of  $\text{Pr}^i\text{NH}_2$  near room temperature is probably due to the hydrolysis of the precursor with a small amount of water in the TG-MS equipment. The precursor is more air-sensitive than  $\text{Nb}(\text{NEt}_2)_4$ ). Laine et al. have reported that the pyrolysis of a TiN precursor with Ti–N( $\text{Pr}^i$ )–Ti imido-bridges led to the evolution of  $\text{C}_3\text{H}_6$  through the direct cleavage of the C–N bond with transfer of  $\beta$ -hydrogen to the nitrogen atom (reaction 3).<sup>20</sup> Since the present precursor possesses M–N( $\text{Pr}^i$ )–M imido-bridges which are very similar to that reported by Laine et al.,  $\text{C}_3\text{H}_6$ , one of the main evolved species, most likely arises from the direct cleavage of the C–N bond via reaction 3, which is different from the formation mechanism of  $\text{C}_2\text{H}_4$  from  $\text{Nb}(\text{NEt}_2)_4$  via the metallacycle intermediate.



Pyrolysis of the precursor under  $\text{NH}_3$  flow at  $600^\circ\text{C}$  for 2 h, and subsequently under  $\text{N}_2$  at  $1350^\circ\text{C}$  for 8 h gave a yellow-gray residue, while a lavender-gray residue was obtained after the pyrolysis under Ar flow at  $1500^\circ\text{C}$  for 2 h. Table 2 shows the ceramic yields, compositional characteristics and the lattice parameters of the pyrolyzed products. The ceramic yields of the precursor are 39.2 and 38.0% for the pyrolyses under  $\text{NH}_3$ – $\text{N}_2$  and Ar flow, respectively. Based on the ceramic yields, the amount of niobium in the precursor, and those in the pyrolyzed products, it can be estimated that 92.7 and 91.1% of the niobium present in the precursor remain in the products pyrolyzed under  $\text{NH}_3$ – $\text{N}_2$  and Ar, respectively. This should be ascribed to the fact that the precursor possesses double niobium–nitrogen bridges as shown in Scheme 1, which makes the degradation of the precursor into smaller volatile Nb-containing species difficult.

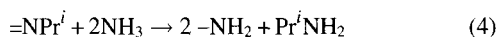


Scheme 2. The main pyrolysis processes for the pyrolysis of  $\text{Nb}(\text{NEt}_2)_4$  in the temperature range of ca.  $160$ –ca.  $280^\circ\text{C}$ .

Table 2. Ceramic Yields and Characteristics of the Products Pyrolyzed under  $\text{NH}_3\text{--N}_2$  (at 600 °C for 2 h under  $\text{NH}_3$ , and then at 1350 °C for 8 h under  $\text{N}_2$ ) and Ar (at 1500 °C for 2 h)

Atmosphere	$\text{NH}_3\text{--N}_2$	Ar
Ceramic yield/%	39.2	38.0
Loss of niobium/%	7.3	8.9
Elemental analysis/mass%		
Nb	83.9	85.1
N	11.2	0.1
C	0.8	16.2
O	3.4	0.3
Total	99.3	101.6
Empirical formula	$\text{NbN}_{0.89}\text{C}_{0.08}\text{O}_{0.23}$	$\text{NbN}_{0.01}\text{C}_{1.47}\text{O}_{0.02}$
Lattice parameter/nm	0.4397	0.4471

After the pyrolysis under Ar flow, a considerable amount of carbon remains in the residue, and the amount of nitrogen is very small (0.1 mass%). In contrast, a considerable amount of nitrogen (11.2 mass%) and a very small amount of carbon (0.8 mass%) are present in the product pyrolyzed under  $\text{NH}_3\text{--N}_2$ . The removal of carbon is probably due to the effective amine-exchange reaction during the pyrolysis under  $\text{NH}_3$ , i.e., two  $\text{--NH}_2$  groups displace one  $\text{=NPr}^i$  group in the precursor and isopropyl amine is liberated.



Removal of carbon during the pyrolysis under  $\text{NH}_3$  due to amine exchange reactions has been reported for other systems such as  $\text{AlN}$  precursors<sup>33</sup> and  $\text{TiN}$  precursors.<sup>34</sup> It should also be noted that 3.4% of oxygen, which was probably introduced during the pyrolysis, is present in the product pyrolyzed under  $\text{NH}_3\text{--N}_2$ .

The pyrolysis of the precursor under  $\text{NH}_3\text{--N}_2$  results in the formation of a NaCl-type compound, but the presence of some weak peaks, which can be assigned to  $\text{NbO}_2$ ,<sup>35</sup> accounts for the presence of oxygen (Fig. 3a). It has been reported that  $\text{NbN}$ ,  $\text{NbC}$ , and  $\text{NbO}$  all possess NaCl-type structures with the lattice parameters of 0.4393,<sup>36</sup> 0.4470,<sup>37</sup> and 0.4211 nm,<sup>38</sup> respectively. Besides, niobium oxynitride  $\text{NbN}_x\text{O}_{1-x}$  also possesses a NaCl-type structure, and the lattice parameter of  $\text{NbN}_x\text{O}_{1-x}$  decreases with the incorporation of oxygen in the lattice; for example  $\text{NbN}_{0.9}\text{O}_{0.1}$  has the lattice parameter of 0.438 nm.<sup>39</sup> The observed lattice parameter of the NaCl-type compound is 0.4397 nm, which is very close to that of  $\delta\text{-NbN}$  (0.4393 nm). Thus, if all the oxygen was present as  $\text{NbO}_2$ , the pyrolyzed product should be a mixture of  $0.89\text{NbN}$  and  $0.11\text{NbO}_2$  based on the empirical formula of  $\text{NbN}_{0.89}\text{C}_{0.08}\text{O}_{0.23}$ .

The pyrolysis of the precursor under Ar leads to the formation of a well-crystallized single-phase NaCl-type compound (Fig. 3b). The observed lattice parameter is 0.4471 nm, which is very close to that of  $\text{NbC}$  (0.4470 nm) rather than that of  $\text{NbN}$  (0.4393 nm). The composition of the product (Table 2) also reveals that the ratios of N/Nb and O/Nb are 0.01 and 0.02 respectively. Thus, the crystallized NaCl-type compound should be cubic  $\text{NbC}$ . The C/Nb ratio of

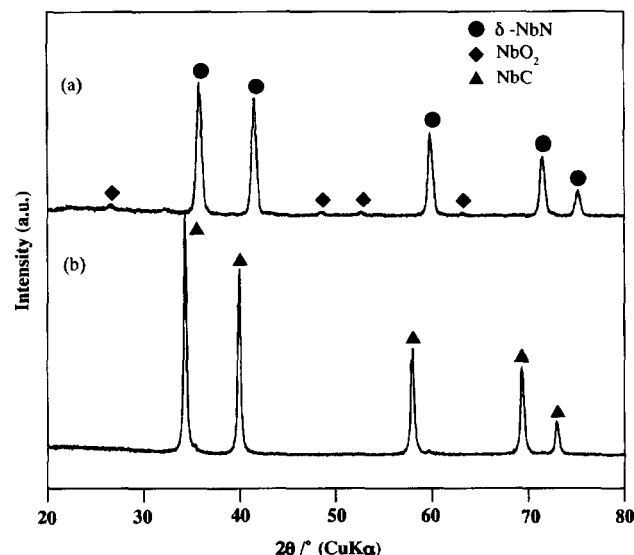


Fig. 3. XRD patterns of the products pyrolyzed under (a)  $\text{NH}_3\text{--N}_2$  (at 600 °C for 2 h under  $\text{NH}_3$ , and subsequently at 1350 °C for 8 h under  $\text{N}_2$ ) and (b) under Ar (at 1500 °C for 2 h).

1.47 (Table 2) suggests that a considerable amount of carbon is present as free carbon. The presence of a large amount of carbon in the residues pyrolyzed under Ar has also been reported during the pyrolysis of titanium precursors prepared with the aminolysis of  $\text{Ti}(\text{NR}_2)_4$ .<sup>19,34</sup>

It is interesting that most of the nitrogen is lost during the pyrolysis under Ar at 1500 °C, although the precursor possesses the initial N/Nb ratio of 2.6. The precursor has also been pyrolyzed at lower temperatures in order to obtain further information about the loss of nitrogen. The compositions of the products are shown in Table 3. After the pyrolysis at 600 °C under Ar, 60.5% of the nitrogen is lost, and very broad peaks ascribable to a NaCl-type compound were observed in the XRD pattern of the residue (not shown). The ceramic yield was 54.5%, close to the ceramic yield of 57% obtained from the TG curve of the precursor (Fig. 2a). Nitrogen is lost mainly as  $\text{Pr}^i\text{NH}_2$  and  $\text{CH}_3\text{CN}$  below ca. 600 °C according to the aforementioned TG-MS analysis

Table 3. Compositional Characteristics of the Products Pyrolyzed under Ar

Temperature/°C	600	1000
Ceramic yield/%	54.5	47.5
Loss of nitrogen <sup>a)/%</sup>	60.5	96.3
Elemental analysis/mass%		
Nb	61.3	68.9
N	10.3	1.1
C	23.6	21.5
O	1.8	2.2
Total	96.8	98.8
Empirical formula	$\text{NbN}_{1.11}\text{C}_{2.98}\text{O}_{0.18}$	$\text{NbN}_{0.19}\text{C}_{2.28}\text{O}_{0.18}$

a) The loss of nitrogen [ $E_{\text{L(N)}}$ ] during the pyrolysis was calculated from the amounts of nitrogen in the precursor [ $W_{\text{P(N)}}$ ] and in the pyrolyzed residues [ $W_{\text{R(N)}}$ ]:  $E_{\text{L(N)}} = [W_{\text{P(N)}} - YW_{\text{R(N)}}]/W_{\text{P(N)}} \times 100$ . Y: ceramic yield.

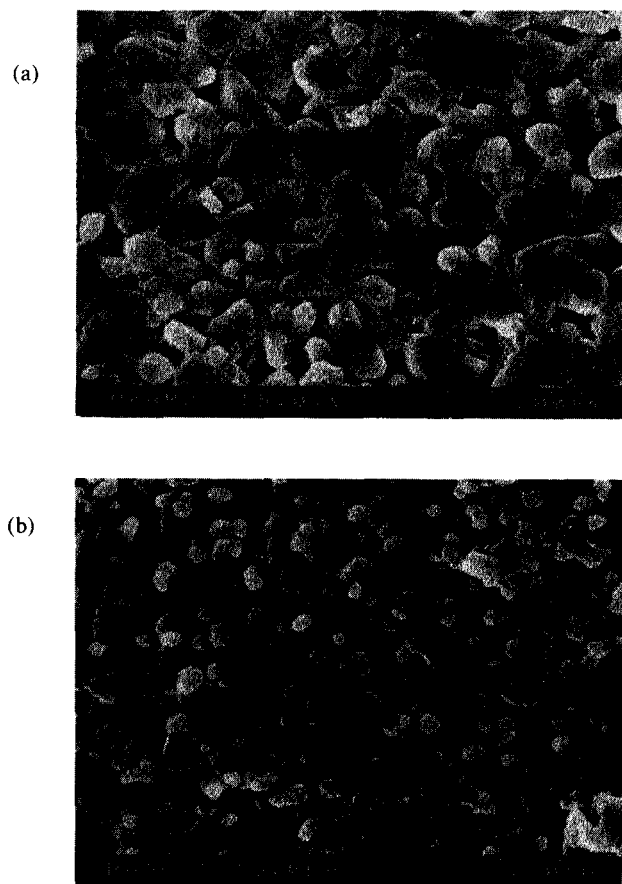


Fig. 4. Scanning electron micrographs of the products pyrolyzed (a) under  $\text{NH}_3\text{--N}_2$  (at 600 °C for 2 h under  $\text{NH}_3$ , and then at 1350 °C for 8 h under  $\text{N}_2$ ) and (b) under Ar (at 1500 °C for 2 h).

results. After the pyrolysis at 1000 °C, a poorly crystalline NaCl-type compound was detected by XRD (not shown). The loss of 96.3% of nitrogen indicates a further loss of nitrogen at 600–1000 °C. The loss of nitrogen during the crystallization from an amorphous phase has also been reported for titanium precursors prepared by the aminolysis of  $\text{Ti}(\text{NMe}_2)_4$ .<sup>20,34</sup>

Scanning electron micrographs of the pyrolyzed products are shown in Fig. 4. Particles with diameters of 0.4–1.0  $\mu\text{m}$  are observed on the surface of the product pyrolyzed under  $\text{NH}_3\text{--N}_2$ . Particles with diameters of 0.1–0.5  $\mu\text{m}$  are observed on the surface of the product pyrolyzed under Ar.

### Summary

The precursor possessing a Nb–N backbone structure was prepared by aminolysis reaction of tetrakis(diethylamido)-niobium with isopropylamine. IR and elemental analysis showed that the precursor was a polymer which contained the Nb–N–Nb imido-bridge structures. The precursor was soluble in benzene. TG-MS analysis and tube pyrolysis showed that the large mass loss, with the evolution of  $\text{C}_3\text{H}_6$ ,  $\text{C}_4\text{H}_8$ ,  $\text{CH}_3\text{CN}$ , and  $\text{Pr}^i\text{NH}_2$  as main species, occurred at a temperature below ca. 500 °C during pyrolysis of the precursor under He. The yellow-gray residue with the ceramic

yield of 39.2% was obtained after pyrolysis of the precursor under  $\text{NH}_3\text{--N}_2$  (at 600 °C for 2 h under  $\text{NH}_3$  and then at 1350 °C for 8 h under  $\text{N}_2$ ), and the XRD analysis indicated that the main crystalline phase was  $\delta\text{-NbN}$ . On the other hand, pyrolysis of the precursor under Ar at 1500 °C for 2 h led to the formation of a lavender-gray residue with the ceramic yield of 38.0%. XRD analysis of the product indicated that NbC was the only crystalline phase. More than 90% of niobium present in the precursor remained in both of the pyrolyzed products. SEM examination showed that the diameters of the particles obtained by pyrolysis under  $\text{NH}_3\text{--N}_2$  and Ar were 0.4–1.0 and 0.1–0.5  $\mu\text{m}$ , respectively.

### References

- 1 L. E. Toth, "Transition Metal Carbides and Nitrides," Academic Press, New York (1971), p. 9.
- 2 P. Ettmayer and W. Lenquauer, in "Encyclopedia of Inorganic Chemistry," ed by R. B. King, John Wiley & Sons, Chichester (1994), p. 2504.
- 3 D. Brown, in "Comprehensive Inorganic Chemistry," ed by J. C. Bailar, H. J. Emeleus, and A. F. Trotman-Dickerson, Pergamon Press, New York (1973), Vol. 3, p. 604.
- 4 H. Abe, K. Hamasaki, and Y. Ikeno, *Appl. Phys. Lett.*, **61**, 1131 (1992).
- 5 T. L. Francavilla, D. L. Peebles, H. H. Nelson, J. H. Claassen, S. A. Wolf, and D. U. Gubser, *IEEE Trans. Magn.*, **23**, 1397 (1987).
- 6 G. Oya and Y. Onodera, *J. Appl. Phys.*, **45**, 1389 (1974).
- 7 R. Fix, R. G. Gordon, and D. M. Hoffman, *Chem. Mater.*, **5**, 614 (1993).
- 8 C. H. Winter, K. C. Jayaratne, and J. W. Proscia, *Mater. Res. Soc. Symp. Proc.*, **327**, 103 (1994).
- 9 C. K. Narula, "Ceramic Precursor Technology and Its Applications," Marcel Dekker, New York (1995).
- 10 G. Pouskoupleli, *Ceram. Int.*, **15**, 213 (1989).
- 11 M. Peuckert, T. Vaahs, and M. Bruck, *Adv. Mater.*, **2**, 398 (1990).
- 12 J. Bill and F. Aldinger, *Adv. Mater.*, **7**, 775 (1995).
- 13 L. Maya, *Inorg. Chem.*, **26**, 1459 (1987).
- 14 G. M. Brown and L. Maya, *J. Am. Ceram. Soc.*, **71**, 78 (1988).
- 15 D. V. Baxter, M. H. Chisholm, G. J. Gama, and V. F. Distasi, *Chem. Mater.*, **8**, 1222 (1996).
- 16 T. Wade and R. M. Crooks, *Chem. Mater.*, **6**, 87 (1994).
- 17 T. Wade and R. M. Crooks, *Chem. Mater.*, **8**, 832 (1996).
- 18 D. C. Bradley and E. G. Torrible, *Can. J. Chem.*, **41**, 134 (1963).
- 19 H. Zheng, K. Oka, and J. D. Mackenzie, *Mater. Res. Soc. Symp. Proc.*, **271**, 893 (1992).
- 20 Y. Liu, D. R. Treadwell, M. R. Kannisto, B. L. Mueller, and R. M. Laine, *J. Am. Ceram. Soc.*, **80**, 705 (1997).
- 21 D. Seyferth and G. Mignani, *J. Mater. Sci. Lett.*, **7**, 487 (1988).
- 22 D. F. Schriver and M. A. Drezdson, "The Manipulation of Air-Sensitive Compounds," 2nd ed, Wiley-Interscience, New York (1986).
- 23 D. C. Bradley and I. M. Thomas, *Can. J. Chem.*, **40**, 449 (1962).
- 24 D. C. Bradley and M. H. Gitlitz, *J. Chem. Soc. A*, **1969**, 980.
- 25 D. C. Bradley and M. H. Chisholm, *J. Chem. Soc. A*, **1971**, 1151.

- 26 C. Airoidi, D. C. Bradley, and G. Vuru, *Transition Met. Chem.*, **4**, 64 (1979). The  $^1\text{H}$ NMR data obtained in this study are as follows:  $\delta$  [ppm] = 1.20 (triplet:  $-\text{CH}_2\text{CH}_3$ ), 3.84 (unresolved:  $=\text{NCH}_2\text{CH}_3$ ) and 3.42 (unresolved:  $-\text{N}(\text{CH}_2\text{CH}_3)_2$ ) for  $(\text{Et}_2\text{N})_3\text{Nb}(\text{=NEt})$ ; 1.03 (triplet:  $-\text{N}(\text{CH}_2\text{CH}_3)_2$ ), 1.45 (triplet:  $-\text{N}(\text{CH})\text{CH}_2\text{CH}_3$ ), 1.80 (doublet:  $=\text{CHCH}_3$ ), 2.49 (quartet:  $=\text{CHCH}_3$ ), 3.84 (unresolved:  $-\text{N}(\text{CH})\text{CH}_2\text{CH}_3$ ), and 3.42 (unresolved:  $-\text{N}(\text{CH}_2\text{CH}_3)_2$ ) for  $(\text{Et}_2\text{N})_3\text{Nb}(\text{EtNCHMe})$ .
- 27 P. P. Power, A. R. Sanger, and R. C. Srivastava, "Metal and Metalloid Amides, -Syntheses, Structures, and Physical and Chemical Properties," Ellis Horwood Limited, Chichester (1980), p. 473.
- 28 K. Kiss-Eross, in "Analytical Infrared Spectroscopy, Comprehensive Analytical Chemistry," ed by G. Svehla, Elsevier, New York (1976), Vol. 5.
- 29 L. M. Dyagileva, V. P. Mar'in, E. I. Tsyganova, I. L. Gaidym, and Yu. A. Aleksandrov, *J. Gen. Chem. USSR*, **50**, 538 (1984).
- 30 Y. Takahashi, N. Onoyama, and Y. Ishikawa, *Chem. Lett.*, **1978**, 525.
- 31 P. Bonnefond, R. Feurer, A. Reynes, F. Maury, B. Chansou, R. Choukroun, and P. Cassoux, *J. Mater. Chem.*, **6**, 1501 (1996).
- 32 R. M. Fix, R. G. Gordon, and D. M. Hoffman, *Chem. Mater.*, **2**, 235 (1990).
- 33 Z. Jiang and L. V. Interrante, *Chem. Mater.*, **2**, 439 (1990).
- 34 S. Koyama, D. Iizuka, Y. Suguhara, and K. Kuroda, *Appl. Organomet. Chem.*, **12**, 787 (1998).
- 35 Powder Diffraction Data File 34-898, JCPDS International Center for Diffraction Data, Swathmore, PA, 1988.
- 36 Powder Diffraction Data File, 38-1155, JCPDS International Center for Diffraction Data, Swathmore, PA, 1988.
- 37 Powder Diffraction Data File, 38-1364, JCPDS International Center for Diffraction Data, Swathmore, PA, 1988.
- 38 Powder Diffraction Data File, 42-1290, JCPDS International Center for Diffraction Data, Swathmore, PA, 1992.
- 39 Powder Diffraction Data File, 25-1360, JCPDS International Center for Diffraction Data, Swathmore, PA, 1988.